Multiple Roles of Component Proteins in Bacterial Multicomponent Monooxygenases: Phenol Hydroxylase and Toluene/ o-Xylene Monooxygenase from Pseudomonas sp. OX1

Multiple Roles of Component Proteins in Bacterial Multicomponent Monooxygenases: Phenol Hydroxylase and Toluene/*o*-Xylene Monooxygenase from *Pseudomonas* sp. OX1[†]

*Christine E. Tinberg, Woon Ju Song, Viviana Izzo, and Stephen J. Lippard**

Department of Chemistry, Massachusetts Institute of Technology, Cambridge, MA 02139

RECEIVED DATE (to be automatically inserted after your manuscript is accepted if required according to the journal that you are submitting your paper to)

[†]This work was funded by grant GM032134 from the National Institute of General Medical Sciences. CET thanks the NIH for partial support under Interdepartmental Biotechnology Training Grant T32 GM08334. VI thanks CEINGE (Biotecnologie Avanzate, Naples, Italy) for partial support.

* To whom correspondence should be addressed. E-mail: lippard@mit.edu. Telephone: (617) 253-1892. Fax: (617) 258-8150.

Running Title: Component Interactions in Bacterial Multicomponent Monooxygenases

ABSTRACT: Phenol hydroxylase (PH) and toluene/*o*-xylene monooxygenase (ToMO) from *Pseudomonas* sp. OX1 require three or four protein components to activate dioxygen for the oxidation of aromatic substrates at a carboxylate-bridged diiron center. In the present study we investigated the influence of the hydroxylases, regulatory proteins, and electron transfer components of these systems on substrate (phenol; NADH) consumption and product (catechol; H_2O_2) generation. Single turnover experiments revealed that only complete systems containing all three or four protein components are capable of oxidizing phenol, a major substrate for both enzymes. Under ideal conditions, the hydroxylated product yield was ~50% of the diiron centers for both systems, suggesting that these enzymes operate by half-sites reactivity mechanisms. Single turnover studies indicated that the PH and ToMO electron transfer components exert regulatory effects on substrate oxidation processes taking place at the hydroxylase actives sites, most likely through allostery. Steady state NADH consumption assays showed that the regulatory proteins facilitate the electron transfer step in the hydrocarbon oxidation cycle in the absence of phenol. Under these conditions, electron consumption is coupled to generation of H_2O_2 in a hydroxylase-dependent manner. Mechanistic implications of these results are discussed.

Bacterial multicomponent monooxygenases (BMMs[1]) are remarkable enzymes that orchestrate a series of electron transfer and substrate activation events in order to prime dioxygen for donation of a

[1] Abbreviations: BMM, bacterial multicomponent monooxygenase; sMMO, soluble methane monooxygenase; AMO, alkene monooxygenase; PH, three component phenol hydroxylase; TMO, four-component alkene/arene monooxygenase; NADH, reduced nicotinamide adenine dinucleotide; MMOH, hydroxylase component of sMMO; MMOB, regulatory protein of sMMO; P*, first peroxodiiron intermediate species of MMOH; H_{peroxo}, second peroxodiiron intermediate species of MMOH; Q, di(μ-oxo)-diiron(IV) intermediate species of MMOH; ToMO, four component toluene/*o*-xylene monooxygenase protein system from *Pseudomonas* sp. OX1; ToMOH, hydroxylase component of ToMO; ToMOD, regulatory protein component of ToMO; RFQ, rapid freeze-quench; PHH, hydroxylase component of *Pseudomonas* sp. OX1 PH; T4mo, four component toluene 4-monooxygenase system from *Pseudomonas mendocina* KR1; MMOR, reductase protein of sMMO; C2,3O, catechol 2,3-dioxygenase; Tris-HCl, 2-amino-2-(hydroxymethyl)-1,3-propanediol hydrochloride; PHM, regulatory protein component of PH; PHP, reductase component of PH; IPTG, Isopropyl β-D-1-thiogalactopyranoside; DTT, dithiothreitol; SDS, sodium dodecyl sulfate; PAGE, polyacrylamide gel electrophoresis; MOPS, 3-(N-morpholino) propanesulfonic acid; ToMOC, Rieske [2Fe-2S] ferredoxin component of ToMO; ToMOF, reductase protein of ToMO; ET, electron transfer; T2MO, toluene 2-monooxygenase system from *Burkholderia cepacia* G4.

single oxygen atom into a C–H bond or across a C=C double bond (*1, 2*). Proteins belonging this family are subdivided into four classes, soluble methane monooxygenases (sMMOs), phenol hydroxylases (PHs), alkene monooxygenases (AMOs), and four-component alkene/arene monooxygenase (TMOs), based on substrate preference and sequence homology (*3, 4*). The ability of BMMs to generate potent oxidizing species without damaging their active sites or consuming electrons in a futile manner depends on the dynamic involvement of three or more protein components: a 200-255 kDa dimeric hydroxylase that houses two copies of a carboxylate-bridged diiron catalytic center; a 38-45 kDa reductase that accepts electrons from NADH and shuttles them though its flavin and [2Fe-2S] cluster cofactors into the hydroxylase diiron sites; and a 10-16 kDa regulatory protein that couples electron consumption to hydrocarbon oxidation (*1, 2, 5*). For ToMO, an additional 12 kDa Rieske protein acts as an electron conduit between the reductase and the hydroxylase. Timely regulation of interactions between these proteins assures efficient catalysis.

The first step in catalysis by the BMM proteins is the reductive activation of O_2 at the hydroxylase diiron centers for incorporation into substrate. The most extensively studied O_2 activation pathways in BMMs are those of the soluble methane monooxygenases (sMMOs) from *Methylococcus capsulatus* (Bath) and from *Methylosinus trichosporium* OB3B. In these systems, reaction of the diiron(II) form of the hydroxylase (MMOH) with O_2 leads to the sequential generation of two peroxodiiron(III) units, P* (*6, 7*) and H_{peroxo} (*8-10*), in the presence of the regulatory protein MMOB. Subsequent transfer of one or two protons (*7, 11*) leads to rearrangement of the iron-oxygen core and formation of Q, a di(μ-oxo)diiron(IV) species responsible for methane oxidation (*8, 12-14*). In the absence of methane and other substrates, Q decays slowly to H_{ox} via a pathway that is not fully understood (*7*).

The O_2 activation pathway of toluene/*o*-xylene monooxygenase (ToMO) from *Pseudomonas* sp. OX1 was also recently investigated (*15*). Upon reaction of the diiron(II) form of the ToMO hydroxylase (ToMOH) with O_2 in the presence of the regulatory protein ToMOD, a diiron(III) intermediate with no obvious absorption features rapidly formed and subsequently decayed to the diiron(III) protein resting state without progressing through a stable, high-valent Q-like intermediate (*15, 16*). The diiron(III)

intermediate, with Mössbauer parameters $\delta = 0.55 \pm 0.02$ mm/s and $\Delta E_Q = 0.67 \pm 0.03$ mm/s, could be a peroxide or hydroperoxide unit (*15*). The spectroscopic characteristics of this species are unusual for a peroxodiiron(III) center, however, which typically exhibits $\lambda_{max} > 650$ nm, $\delta > 0.6$ mm/s, and $\Delta E_Q > 1.0$ mm/s. These notable differences suggest that the ToMO intermediate must deviate in geometry and/or protonation state from well characterized diiron(III) peroxide species, but its exact nature remains to be fully elucidated. This species is believed to be the active oxidant in the ToMO system, because rapid freeze quench (RFQ) double-mixing Mössbauer spectroscopic experiments revealed that its rate of decay is accelerated in the presence of the substrate phenol (*15*). Analogous investigations of the O_2 activation pathway of the hydroxylase component from *Pseudomonas* sp. OX1 phenol hydroxylase hydroxylase component (PHH) revealed a similar intermediate species in this enzyme (*17*).

Although the hydroxylase proteins have been definitively established to house the diiron catalytic reaction centers, the functions of the regulatory proteins of BMMs have been a source of ongoing investigation. These proteins, of which the best-studied is MMOB in sMMO, have been implicated in the O_2 activation, substrate entry, proton transfer, and electron transfer phases of the catalytic cycles for hydrocarbon oxidation (*1, 2, 18*). The regulatory proteins increase the rates and electron coupling efficiencies of the steady-state hydroxyation reactions (*19-22*), modulate the redox potentials of the hydroxylase diiron site (*23, 24*), accelerate the rates of electron transfer between the reductase and the hydroxylase (*20, 21*), perturb the spectroscopic features of the hydroxylase active site (*19, 25-29*), rearrange the hydroxylase iron ligands (*28, 30, 31*), promote conformational changes in the hydroxylase (*21, 28, 30-33*), gate substrate and solvent access to the hydroxylase diiron centers (*30, 34*), alter the substrate specificity and regiospecificity of hydroxylation reactions (*27, 34-36*), promote the binding of an active site water molecule invoked in proton transfer (*30*), modulate the kinetics of the reaction of reduced hydroxylase with O_2 (*37*), and prevent inopportune reduction of the oxygenated iron intermediates of the hydroxylase via untimely electron transfer (*30-32, 38*). At high concentrations, the regulatory proteins inhibit steady state activity in the sMMO, PH, and toluene 4-monooxygenase (T4mo) systems (*19, 20, 39*). The ability of these small, cofactorless proteins to influence so many

distinct processes clearly indicates a mechanistic complexity that is not yet fully understood. Further studies of these and other BMM regulatory components are necessary to obtain a complete picture of their functions.

Reductase protein components in the BMM systems provide electrons to the diiron centers in the hydroxylases (*1, 2*). The sMMO reductase MMOR, however, also affects catalysis in a complicated and versatile manner, tuning the redox potentials of the hydroxylase diiron units (*23, 38*), altering the kinetics of the reaction with O_2 (*38*), promoting conformational changes in the hydroxylases (*32, 33*), and influencing how the hydroxylases interact with substrates (*27*). These observations suggest that MMOR regulates catalysis in addition to providing electrons for the reductive activation of dioxygen. Whether or not this phenomenon is restricted to sMMO, or is a general feature of all BMMs, is of interest to establish and has motivated in part the present investigation.

Toluene/*o*-xylene monooxygenase and phenol hydroxylase are the first two enzymes in a pathway that allows *Pseudomonas* sp. OX1 to metabolize aromatics as its sole carbon source (Scheme 1). Enzymes involved in the upstream segment of this pathway, ToMO, PH, and catechol 2,3-dioxygenase (C2,3O), degrade aromatic molecules through oxidation reactions. Downstream '*meta*-cleavage' enzymes then cleave the modified aromatic ring and process the resulting products for entry into major metabolic pathways required for bacterial viability (*39, 40*). Both ToMO and PH have a broad substrate specificity and oxidize a variety of aromatic hydrocarbons in addition to their native substrates, including *o*-, *m*-, and *p*-cresol, several dimethylphenols, and benzene (*39, 41*). By comparison to the sMMO systems, little is known about how the protein components of the *Pseudomonas* sp. OX1 BMMs act together to achieve hydrocarbon oxidation. In the studies undertaken here, we explored the influences of the *Pseudomonas* sp. OX1 PH and ToMO auxiliary proteins on substrate (phenol; NADH) consumption and product (catechol; H_2O_2) formation. The results and their interpretation constitute the present report.

MATERIALS AND METHODS

General Considerations. Distilled water was deionized with a Milli-Q filtering system. Tris-HCl gradient gels (4-20%) were purchased from Bio-Rad Laboratories. Phenol and catechol were purified by vacuum-sublimation prior to use. Other reagents were purchased from Sigma Aldrich and used as received unless otherwise noted.

Protein Purification. PHH was expressed from a vector containing the *phk*, *phl, phn,* and *pho* genes (pGEM3Z/PHΔMΔP). Construction of this plasmid, as well as expression and purification of hydroxylase protein from this construct, will be described elsewhere (*17*). Plasmids containing the genes for the PH regulatory protein, PHM (pET22b(+)/PHM), and reductase, PHP (pET22b(+)/PHP), were supplied by Prof. Alberto Di Donato (Università di Napoli Federico II, Naples, Italy). PHP was expressed as described previously, except that $Fe(NH_4)_2(SO_4)_2 \cdot 6H_2O$ and IPTG were added to final concentrations of 200 μM and 75 μM, respectively, at induction (*39*). The resulting cell paste (~20 g) was sonicated on ice using a Branson sonifier in 30 s pulses for 12 min at 40% output in ~100 mL of 20 mM sodium phosphate pH 7.0, 1 mM DTT, and 10% glycerol (Buffer A) containing 100 U of DNaseI (New England Biolabs). Insoluble material was removed by ultracentrifugation at 183,000 x *g* for 60 min, and the supernatant was filtered through a 0.45 μm membrane and loaded onto a Q Sepharose FF column (100 mL) equilibrated in Buffer A. The column was washed with 200 mL of Buffer A, after which bound proteins were eluted in 1 L by running a linear gradient from 0.08 to 1.0 M NaCl at 1.5 mL/min. Fractions containing PHP eluted at ~350 mM NaCl and were identified by SDS-PAGE gel electrophoresis and by absorbance at 271, 340, and 459 nm. These fractions were pooled and concentrated to ~7 mL using a 30K MWCO Amicon centrifugal concentrator (Millipore). The resulting protein was loaded onto a Superdex S75 column equilibrated with Buffer A containing 0.2 M NaCl (Buffer B). Proteins were eluted by running Buffer B over the column at a flow rate of 1 mL/min. Fractions displaying an A_{271}:A_{459} ratio of 2.5 to 3 and an A_{340}:A_{459} ratio slightly lower than one and

appearing pure by SDS-PAGE were pooled, concentrated, flash-frozen in liquid nitrogen, and stored at -80 °C until further use.

PHM was expressed as described previously (*39*). The resulting cell paste was sonicated on ice using a Branson sonifier in 30 s pulses for 12 min at 40% output in ~100 mL of 25 mM MOPS pH 7.0, 10% glycerol (Buffer C) containing 100 U of DNaseI (New England Biolabs). Insoluble material was removed by ultracentrifugation at 183,000 x *g* for 60 min., and the supernatant was filtered through a 0.45 μm membrane and loaded onto a Q Sepharose FF column (100 mL) equilibrated in Buffer C. The column was washed with 200 mL of Buffer C, after which bound proteins were eluted in 1 L by running a linear gradient from 0 to 0.5 M NaCl at 1.5 mL/min. PHM eluted in two peaks centered around at ~340 and ~400 mM NaCl that were identified by monitoring the absorbance at 280 nm and by SDS-PAGE and native gel electrophoresis. The contents of fractions corresponding to the first, the second, or both peaks were pooled and concentrated to ~7 mL using a 3K MWCO Amicon centrifugal concentrator (Millipore). The resulting protein was loaded onto a Superdex S75 column equilibrated with Buffer C containing 0.2 M NaCl (Buffer D). Proteins were eluted by running Buffer D over the column at a flow rate of 1 mL/min. PHM eluted in one broad peak with a shoulder. Fractions appearing pure by SDS-PAGE were pooled and concentrated. Properly folded PHM was obtained by thermally denaturing the protein and then letting it refold by slowly cooling the solution to room temperature. For this process, PHM was diluted to 75 μM in 25 mM MOPS, pH 7.0, containing 10% glycerol. The protein was heated to 70 °C over 30 min in a water bath, then the bath was removed from the heating block and the protein allowed to cool until it reached room temperature. The resulting protein was analyzed by native gel electrophoresis, flash-frozen in liquid nitrogen, and stored at -80 °C until further use.

The hydroxylase, ToMOH (*42*), regulatory, ToMOD (*43, 44*), Rieske, ToMOC (*42*), and reductase, ToMOF (*45*), components of ToMO and the ToMOH I100W variant (*16, 46*) were purified as described previously. Specific activities of both PH and ToMO were measured using a coupled assay employing catechol 2,3-dioxygenase and phenol as a substrate (*42*). Hydroxylase iron content was determined by

the ferrozine colorimetric assay (*47*). Using these procedures, we typically obtained protein activity in the range of 1200-1400 mU/mg for PHH and of 1100-1300 mU/mg for ToMOH, and the iron contents ranged from 3.6-4.1 Fe atoms per dimer for PHH and 3.9-4.1 Fe atoms per dimer for ToMOH. Approximate extinction coefficients used to quantify the PH hydroxylase, regulatory, and reductase proteins were calculated from primary amino acid sequences as 600,000 M^{-1} cm^{-1}, 12,000 M^{-1} cm^{-1}, and 21,000 M^{-1} cm^{-1}, respectively, at 280 nm. Approximate extinction coefficients used to quantify the ToMO hydroxylase and regulatory proteins, calculated from primary amino acid sequences, were 600,000 M^{-1} cm^{-1} and 2,860 M^{-1} cm^{-1}, respectively, at 280 nm. Extinction coefficients used to quantify the ToMO reductase and Rieske protein were previously reported (*42*).

Single Turnover Assays. For all assays, the appropriate protein mixture prepared in 400 μL of 0.1 M Tris-HCl, pH 7.5, was reduced in an anaerobic chamber by addition of a stoichiometric quantity of sodium dithionite or on the benchtop by the addition of stoichiometric NADH. Accurate $Na_2S_2O_4$ concentrations were determined by anaerobic titration into $K_3[Fe(CN)_6]$ (*48*). For studies probing PH, reaction solutions contained 100 μM PHH, 0 or 600 μM PHM, 10 or 200 μM PHP, 5 mM phenol, and 200 μM NADH or $Na_2S_2O_4$. For experiments monitoring ToMO, reaction solutions contained 50 μM ToMOH, 0 or 100 μM ToMOD, 100 μM ToMOC, 5 μM ToMOF, 500 μM phenol, and 50 μM NADH or $Na_2S_2O_4$. For studies investigating the influence of the cognate electron transfer protein on O_2 activation, a solution containing hydroxylase, phenol, and regulatory protein if used was pre-reduced with stoichiometric $Na_2S_2O_4$ for 20 min before the addition of oxidized electron transfer protein (PHP or ToMOC). Following removal from the glove box, 100 μL of O_2-saturated buffer was added to each solution. Reaction mixtures were incubated for 20 min at 25 °C, after which they were quenched by addition of 100 μL of 0.4 M TCA. Precipitated protein was removed by centrifugation at 17,110 x *g* for 10 min and the supernatant was assayed for catechol content by HPLC.

HPLC experiments were performed on a Vydac C_{18} reversed-phase protein and peptide column thermostatted at 25 °C. Absorbance of the eluent was monitored continuously at 280 and 274 nm. The separation program utilized a 1 mL/min flow rate with a two-solvent system step gradient consisting of

0.1% HCOOH in ddH_2O (solvent A) and 0.1% HCOOH in methanol (solvent B). HPLC separations first employed an isocratic elution with 2% B for 10 min that was followed by a linear gradient from 2% to 98% B over 10 min. The column was then flushed with 98% B for 10 min followed by a linear gradient from 98% to 2% B over 1 min. Finally, 2% B was run over the column for 15 min to prime it for the next run. A 100 μL aliquot of sample was injected on the column for each run. Under these conditions, phenol and catechol eluted at 18.5 and 10.1 min, respectively. Peaks corresponding to phenol or catechol were integrated and the phenol or catechol content was measured by comparison to a standard curve prepared in the same manner as the test solutions. All experiments were run in triplicate using enzymes prepared from different batches of cell paste. Standard curves were run each time the assay performed.

H_2O_2 Production Assays. H_2O_2 was detected using a modified version of a discontinuous colorimetric assay employing KSCN and $Fe(NH_4)_2(SO_4)_2{\cdot}6H_2O$ (*49*). However, this procedure had to be changed because NADH interfered with the assay. A step was therefore added to inactivate the reducing agent prior to assaying the reaction mixtures. For studies monitoring PH, reaction solutions contained 1 μM PHH, 0 or 6 μM PHM, 0.1 or 2 μM PHP, and 200 μM NADH in 500 μL of 0.1 M Tris-HCl, pH 7.5. For reactions probing ToMO, reaction solutions contained 1 μM ToMOH, 0 or 2 μM ToMOD, 2 μM ToMOC, 0.1 μM ToMOF, and 200 μM NADH in 500 μL of 0.1 M Tris-HCl, pH 7.5. PH and ToMO reaction mixtures also contained 10 μM of the *E. coli* catalase inhibitor NH_2OH (*50*) to eliminate a trace catalase impurity activity, which has been shown to affect previous BMM H_2O_2 assays performed with recombinant proteins (*22, 51*). For reactions employing substrate, the concentration of phenol was 5 mM. All reactions were performed at 25.0 ± 0.1 °C or 4.0 ± 0.5 °C. Reactions were initiated by addition NADH and were quenched after a specified reaction time by addition of 100 μL of 0.4 M TCA. To inactivate unconsumed NADH, acid-quenched reaction mixtures were placed in a water bath at 90 °C for 15 min, then removed and allowed to cool to room temperature for 45 min prior to separation of the protein precipitate by centrifugation at 17,110 x *g* for 5 min. Following centrifugation, 500 μL of supernatant was transferred to a fresh Eppendorf tube. A 200 μL portion of 10 mM

$Fe(NH_4)_2(SO_4)_2 \cdot 6H_2O$ prepared in ddH_2O and 100 μL of 2.5 M KSCN dissolved in ddH_2O were added to each Eppendorf tube. The reaction mixtures were stirred and allowed to stand for 5 min before their absorption at 480 nm was monitored. Solutions of H_2O_2 in buffer were treated in the same manner as the enzyme reactions to generate a standard curve. For the standards, the concentration of a freshly prepared H_2O_2 stock solution was determined by measuring the absorbance at 240 nm (ε_{240} = 43.6 M^{-1} cm^{-1}) (*52*). Data displaying hyperbolic H_2O_2 generation kinetics were fit to the exponential growth model y = A*exp(-*k*t) + B to obtain the first-order rate constant for H_2O_2 production.

H_2O_2 and NH_2OH Inactivation Assays. Two methods were used to assay for inactivation of PH by H_2O_2. In the first, reaction solutions containing 0.5 μM PHH, 3 μM PHM, and 1 μM PHP in 500 μL of 0.1 M Tris-HCl, pH 7.5 were incubated with 0 or 50 μM H_2O_2 and 1 mM phenol for 20 min. Subsequently, 1 mM NADH was added to initiate the hydrocarbon oxidation reaction. These reactions were quenched after a specified time by the addition of 100 µL 0.4 M TCA. In the second method, reaction solutions containing 1 μM PHH, 6 μM PHM, and 2 μM PHP in 500 μL of 0.1 M Tris-HCl, pH 7.5 were incubated with 5 mM NADH for a specified time period, after which phenol was added to a final concentration of 5 mM. Reactions were allowed to proceed for 20 min and then were quenched by the addition of 100 µL of 0.4 M TCA. For both methods, precipitated protein was removed by centrifugation at 17,110 x *g* for 10 min. Following centrifugation, 400 μL of supernatant was transferred to an HPLC vial and the samples were assayed for catechol content as described above. For the first method, activity was assessed by plotting the amount of catechol formed versus time incubated with H_2O_2 and fitting those data to the linear equation y = *k*x + b. For the second method, data were plotted as the percentage of the amount of catechol formed in experiments in which NADH and phenol were added simultaneously (*t* = 0 min) versus the time that the reaction mixture was incubated with NADH before addition of phenol.

To determine whether addition of the *E. coli* catalase inhibitor NH_2OH affects enzyme activity of PH or ToMO, HPLC-based activity assays were performed in its presence and absence. For PH, reaction

solutions contained 2 μM PHH, 12 μM PHM, 4 μM PHP, 1 mM phenol, and 0 or 20 μM NH_2OH in 250 μL of 0.1 M Tris-HCl, pH 7.5. Aliquots of 350 μM NADH were added to initiate hydrocarbon oxidation. Reactions were quenched after 2 or 10 min by addition of 100 μL 0.4 M TCA, and precipitated protein was removed by centrifugation at 17,110 x *g* for 10 min. Following centrifugation the samples were assayed for catechol content by HPLC as described above. For ToMO, reaction solutions contained 1 μM ToMOH, 4 μM ToMOD, 2 μM ToMOC, 0.1 μM ToMOF, 2 mM phenol, and 0 or 10 μM NH_2OH in 500 μL of 0.1 M Tris-HCl, pH 7.5. Aliquots of 500 μM NADH were added to initiate hydrocarbon oxidation. Reactions were quenched after 1, 5 or 15 min after reaction initiation by addition of 100 μL of 0.4 M TCA, and precipitated protein was removed by centrifugation at 17,110 x *g* for 10 min. Following centrifugation the samples were assayed for catechol content by HPLC as described above.

H_2O_2 Consumption Assays. H_2O_2 consumption by PH was monitored using the discontinuous colorimetric assay described above without the NADH inactivation step. Reaction mixtures contained 0 or 1 μM PHH, 0 or 6 μM PHM, 2 μM PHP, and 1 mM phenol in 500 μL of 0.1 M Tris-HCl, pH 7.5. Reactions were initiated by addition of 10 or 50 μM H_2O_2 and were quenched after specified reaction times with 100 μL of 0.4 M TCA. Precipitated protein was removed by centrifugation at 17110 x *g* for 5 min. Following centrifugation, 500 μL of supernatant was transferred to a fresh Eppendorf tube, and the reaction mixtures were assayed for H_2O_2 content.

NADH Consumption Assays. NADH consumption was monitored continuously by absorbance at 340 nm (ε_{340} = 6220 M^{-1} cm^{-1}). For studies probing PH, reaction mixtures contained 0 or 1 μM PHH, 0 or 6 μM PHM, 0.1 or 2 μM PHP, and 200 μM NADH in 600 μL of 0.1 M Tris-HCl, pH 7.5. For experiments monitoring ToMO, reaction solutions contained 0 or 1 μM ToMOH, 0 or 2 μM ToMOD, 2 μM ToMOC, 0.1 μM ToMOF, and 200 μM NADH in 500 μL of 0.1 M Tris-HCl, pH 7.5. For reactions containing substrate, the concentration of phenol was 5 mM. All reactions were initiated by addition of

PHP for PH and NADH for ToMO. Reactions were thermostatted at 25.0 ± 0.1 °C using a circulating water bath. Data were analyzed by fitting the initial time points to the linear function $y = kx + b$.

RESULTS

Toluene/*o*-xylene monooxygenase (ToMO) and phenol hydroxylase (PH) from *Pseudomonas* sp. OX1 are BMMs responsible for catalyzing the first two steps in the metabolism of benzene, phenol, and other aromatics that can serve as the sole source of carbon and energy for the organism. To understand better the manner in which ToMO and PH utilize a carboxylate-bridged diiron center to hydroxylate aromatic molecules, we conducted a series of studies aimed at investigating the multiple roles of the component proteins in these systems. In all assays, the ratios of protein components employed were those that are reported and verified in our laboratory to yield maximal catechol formation rates in steady state experiments. For ToMO, maximal product formation rates occur when 2 equiv of regulatory protein ToMOD, 2 equiv of Rieske protein ToMOC, and 0.1 equiv of reductase ToMOF are present per hydroxylase molecule (*42*). For most studies, 2 equiv of ToMOD per ToMOH were used; however, because ToMOD does not inhibit steady state activity as noted for other BMM regulatory proteins (*42*), experiments employing higher ratios of ToMOD were also conducted and are directly comparable to those employing 2 equiv of ToMOD. For PH expressed from the pGEM3Z/PHΔMΔP vector and used throughout these studies, maximal product formation occurred when ~ 6 equiv of PHM (Figure S1a) and 2 equiv of PHP (data not shown) are present per hydroxylase molecule. In contrast to ToMOD, excess PHM does inhibit enzyme activity.

S*ingle Turnover Assays*. First we quantified the amount of catechol formed by various component mixtures during enzyme single turnover using phenol as the substrate (Table 1). A negligible amount of catechol (<10% per diiron sites) was formed when the hydroxylase proteins PHH or ToMOH were reduced with $Na_2S_2O_4$ in the absence of their respective auxiliary proteins. Addition of these regulatory proteins, PHM or ToMOD, to the cognate hydroxylase did not significantly enhance product yield. For PH, addition of the reductase (PHP) to PHH improved the product yield, although the amount of

catechol formed is probably too low to be physiologically relevant. In similar experiments, the ToMO Rieske protein, ToMOC, did not substantially affect the amount of product formed by ToMOH. Only the fully coupled systems containing the hydroxylase, regulatory protein, reductase, and Rieske protein for ToMO were able to generate a significant amount of product. For both PH and ToMO, ~50% of phenol with respect to protein active site clusters was converted to catechol when stoichiometric NADH or $Na_2S_2O_4$ was used as the reductant, even though the substrate was present in great excess.

To investigate whether the electron transfer (ET) proteins exert regulatory effects on their corresponding hydroxylases in a manner that influences the product yield, single turnover experiments were conducted in which a hydroxylase/regulatory protein mixture was reduced with stoichiometric $Na_2S_2O_4$ for 20 min prior to addition of oxidized reductase (PHP) for PH or Rieske protein (ToMOC) for ToMO. Quantitation of catechol formed after solutions oxygenation revealed significant enhancements in product yield from the hydroxylase-regulatory protein complex. This ET protein-promoted enhancement in catechol formation was larger for PH than for ToMO, the latter generating three times more product in the presence of oxidized ToMOC than in its absence. It is important to note that maximal (~50%, vide infra) product accumulation did not occur under these conditions for either enzyme system, however.

Steady State NADH Consumption by PH and ToMO. We also examined the effects of the auxiliary proteins on steady state catalysis. Table 2 shows the rates of NADH consumption during steady state turnover in the PH and ToMO systems under a variety of conditions. PHH and ToMOH do not consume NADH in the absence of their cognate ET proteins. The rate of ET from the reductase/Rieske to the hydroxylases is accelerated by two- to three-fold in the presence of the regulatory protein in both systems, a phenomenon also observed in sMMO (*20*). As expected, the rates of NADH consumption are significantly enhanced by the presence of phenol. Similar trends in the NADH consumption rates were observed for PH at 4 °C (data not shown).

Steady State H_2O_2 Production PH and ToMO. In the absence of hydrocarbon substrate, some BMM systems generate H_2O_2 catalytically (*15, 20, 51*). Production of H_2O_2 might result from two sources: (i) protonation and liberation from peroxodiiron(III) intermediates generated at the hydroxylase diiron active sites during O_2 activation in the absence of hydrocarbon (*15, 17*), and/or (ii) oxidase activity of the ET protein(s). To determine the mechanism(s) of H_2O_2 generation, we measured the ability of various protein mixtures to produce this molecule. The *E. coli* catalase inhibitor NH_2OH was added in all assays to prevent competing H_2O_2 generation or consumption by trace *E. coli* catalase impurities (*51*). A control experiment indicated that NH_2OH does not interfere with the enzymatic activity of PH or ToMO. Steady state assays performed in the presence and absence of NH_2OH yielded identical amounts of catechol at several time points ranging from one to 15 min after reaction initiation (data not shown).

Initial attempts to quantify H_2O_2 production by PH and ToMO employed a colorimetric method that measures the oxidation of Fe(II) by H_2O_2 by monitoring complexation of the resulting Fe(III) ion with thiocyanate ion (*49*). However, this procedure had to be modified because NADH interferes with formation of the colored isothiocyanatoiron(III) complex in a complex manner (Figure S2a). A method was therefore developed to inactivate the reducing agent following reaction quenching but prior to H_2O_2 analysis. Although H_2O_2 is reasonably stable to heat for short time periods (~ 1 hr) under acidic conditions, NADH can be inactivated when exposed to low pH and elevated temperatures (*53*). Accordingly, the quenched reaction mixtures were heated to 90 °C for 15 min and then cooled to room temperature over a period of 45 min before the precipitated protein was removed by centrifugation and the supernatant was assayed for H_2O_2 content. Using this method, a hydrogen peroxide standard curve was found to be independent of NADH concentration (Figure S2b). This procedure was therefore employed in all H_2O_2 detection experiments performed in the presence of NADH.

With this revised method, we conducted steady state assays that revealed H_2O_2 evolution from the complete PH (Figure 1a) and ToMO (Figure 1b) systems in the absence of phenol but not in its presence. In the presence of phenol H_2O_2 is probably not formed because electron consumption is fully coupled to hydrocarbon oxidation. The H_2O_2 evolution profiles of PH and ToMO generated in the

absence of phenol displayed hyperbolic behavior with non-zero y-intercepts. The small amount of apparent H_2O_2 present in the assay mixtures at time zero probably results from protein-bound iron(III) that dissociates upon precipitation and then binds to thiocyanate in the reaction mixture to form isothiocyanatoiron(III) and produce the red color detected. Accordingly, the values on the y-intercept correspond approximately to the iron content of the proteins being assayed. Fits of the H_2O_2 profiles to single exponential processes returned first-order rate constants of 1.8 min^{-1} for PH and 6.8 min^{-1} for ToMO. It is important to note for these studies that PH does not consume H_2O_2 in the absence of hydrocarbon substrate. Assays employing NH_2OH and either a 10- or 50-fold excess of H_2O_2 indicated no consumption of hydrogen peroxide by the enzyme system over an 8 min period in the absence (Figure S3a) or presence (Figure S3b) of PHM. Given these findings, reports that both ToMOH (*15*) and toluene 2-monooxygenase (T2MO) from *Burkholderia cepacia* G4 (*54*) can consume H_2O_2 by means of catalase activity are likely to reflect small amounts of catalase protein contaminants rather than hydroxylase activity as a catalase (*22, 51*).

The observed hyperbolic behavior of the H_2O_2 evolution profiles is most likely due to enzyme inactivation by the hydrogen peroxide that is generated, as previously reported for phenol hydroxylase from *Pseudomonas* sp. CF600 (*55*). To examine whether PH is indeed inactivated over the course of the reaction, we treated the enzyme system with NADH for time periods between 1 and 8 min before adding phenol. The resulting mixture was incubated for 20 min and then analyzed for catechol content. Catechol yield decreased as a function of NADH-enzyme incubation time, indicating that time-dependent protein inactivation occurs under the conditions employed in the steady state H_2O_2 assays (Figure 2). To determine whether the observed enzyme inactivation could be mediated by formation of H_2O_2, the enzyme system was incubated with a 100-fold excess of H_2O_2 for 20 min prior to assaying for catechol content. HPLC quantification revealed that the H_2O_2-exposed system generated only 63% of the catechol observed for the untreated enzyme. Together, these results indicate that the hyperbolic nature of the H_2O_2 generation curve results from enzyme inactivation by H_2O_2. We note that the enzyme inactivation process observed in these studies seems to occur more slowly than the H_2O_2 generation

curve plateaus, but argue that the results of the two experiments can only be compared qualitatively and not quantitatively because of inherent differences in experimental conditions, most notably the type of product monitored. The mechanism of enzyme inactivation probably stems from H_2O_2-mediated free radical damage to the PH proteins. Similar behavior is expected for ToMO (*15*).

To delineate the mechanism of H_2O_2 production by PH, we examined the abilities of the reductase and hydroxylase to independently generate it. PHP produces H_2O_2 in the presence of O_2 and NADH (Figure 3a). The reaction is characterized by hyperbolic H_2O_2 evolution, and a fit of the data to an exponential growth model revealed a first-order rate constant k of 0.82 min^{-1}. Under similar conditions, PHP does not consume H_2O_2 in the absence of NADH (Figure S4). The measured rate of H_2O_2 formation by two equiv of PHP is insufficient to account for the H_2O_2 formed by the complete enzyme system, however. It is therefore likely that H_2O_2 arises instead from PHH or from PHH *and* PHP. To distinguish between these two possibilities, H_2O_2 assays were performed with PHH, 6 equiv of PHM, and 0.1 equiv of PHP. At this sub-stoichiometric ratio of PHP to PHH, electron consumption and product formation are fully coupled (*39*) and H_2O_2 will not be generated by oxidase activity of the reductase protein. These conditions led to H_2O_2 release from the hydroxylase in a hyperbolic fashion with a first-order rate constant k of 0.77 min^{-1} (Figure 3b). However, the rate of H_2O_2 production under these conditions is also insufficient to account for the H_2O_2 generation profile observed in the presence of the complete, stoichiometric enzyme system. We therefore conclude that H_2O_2 arises from *both* PHP oxidase activity and from generation at the hydroxylase diiron centers under the conditions employed.

In contrast to PH, H_2O_2 evolution from ToMO occurs only from the hydroxylase diiron center. Because these experiments employed sub-stoichiometric amounts of reductase (ToMOF) and because ET from ToMOC to ToMOH is rapid (*56*), it is unlikely that H_2O_2 results from oxidase activity of the ET proteins. The H_2O_2 evolution profile of ToMOH I100W, a variant having a tryptophan residue installed near the enzyme active site, displays a significantly decreased rate of H_2O_2 formation, with k = 0.84 min^{-1}, and a marked decrease in the total amount of H_2O_2 generated relative to that of the wild-type protein (Figure 4). The peroxodiiron(III/III) intermediate of ToMOH I100W generated during O_2

activation decays via a one electron-transfer pathway to form a W• and a mixed-valent diiron(III/IV) species (*46*) rather than directly proceeding to the the diiron(III) resting enzyme state as observed for wild-type protein (*15*). The diminished amount of H_2O_2 produced by ToMOH I100W is attributed to this competing process of intermediate decay, which will not produce H_2O_2.

DISCUSSION

The remarkable ability of BMM systems to perform challenging hydrocarbon oxidation reactions in a regioselective manner depends on the coordinated efforts of three or more protein components. Regulation of the dynamic interplay between these proteins is crucial to maintaining effective and sustainable enzyme systems. However, these protein interactions are complicated and the functions of the individual protein components are still not fully understood.

Evidence for Half-Sites Reactivity in PH and ToMO. The observations that the complete PH or ToMO systems generate ~50% of product per active sites in single turnover assays (Table 1) and that fewer than 50% of the diiron sites proceed though the common peroxodiiron(III) intermediate thought to be responsible for arene oxidation during O_2 activation (*15, 17*) indicate that these proteins react by a half-sites reactivity mechanism. In this model, negative cooperativity between the two active site protomers assures a mechanism in which only one subunit of the dimer activate O_2 at a time. Such allosteric communication ensures that the other active site is simultaneously engaged in the reductive phase of the catalytic cycle. In support of this mechanism, the crystal structure of the PHH/PHM complex revealed a regulatory protein bound only at one side of the hydroxylase dimer (*31*), suggesting that one active site in the dimer proceeds through the catalytic cycle at a time[2]. In contrast, MMOH does not proceed by a half-sites type of mechanism, because 90-100% of product forms per diiron sites in single turnover assays (*38*).

[2] X-ray crystal structures of oxidized and reduced hydroxylase-regulatory protein complexes from *Pseudomonas mendocina* KR1 toluene 4-monooxygenase reveal one equiv of regulatory protein bound to each protomer of the hydroxylase, however (Bailey, L. J., McCoy, J. G., Phillips Jr., G. N., and Fox, B. G. (2008) *Proc. Natl. Acad. Sci. USA 105*, 19194-19198). The reason for this difference is unknown.

Electron Transfer Proteins Regulate Hydroxylase Chemistry. Single turnover experiments reveal that BMM electron transfer proteins affect the O_2 activation/substrate oxidation steps of catalysis as well as reducing the hydroxylase diiron sites, because the product yield is greatly enhanced by the presence of these proteins even when ET is not operative (Table 1). This conclusion is highlighted by results from single turnover assays in which addition of oxidized ET protein to a pre-reduced hydroxylase/regulatory protein mixture generated more product than that obtained from reduced hydroxylase/regulatory protein (Table 1). Although maximal (~50%, vide infra) catechol accumulation does not occur under these conditions, the amount of product formed is significantly greater than that generated in the absence of the appropriate ET protein. Because ET from the reductase to the hydroxylase should not occur under these conditions, the enhancement in product yield must arise solely from allosteric effects. The mechanism(s) by which the electron transfer protein regulates phenol oxidation is unknown; however, studies from sMMO suggest that the binding of MMOR induces a long-lived conformational change in MMOH (*27, 32, 33*) and that MMOR modulates product regiospecificity, presumably by altering hydroxylase-substrate interactions (*27*). The PH and ToMO ET proteins might therefore affect hydroxylase activity by opening a conformationally responsive substrate gate. In the presence of the appropriate electron transfer protein, the hydroxylase would assume a conformational setting in which hydrocarbon substrates can more readily access the active site. Recent structural studies of the T4mo hydroxylase/regulatory protein (*30*) indicate that hydrocarbon substrate must enter the active site prior to binding of the regulatory protein, before or during reduction of the hydroxylase, adding further support for this argument.

The regulatory roles of the ET proteins have a more marked effect in PH and ToMO than in sMMO, because single turnover product yields are more significantly affected by the presence of the regulatory protein than in sMMO. PHH or ToMOH alone cannot catalytically generate a significant amount of product; however, reduced sMMO hydroxylase, MMOH, produces ~40% propylene oxide per diiron sites in single turnover reactions using propylene as substrate and ~80% in the presence of the regulatory protein, MMOB (*38*). MMOR also slightly enhances the product yield in these experiments.

Addition of 0.5 equiv of MMOR to a mixture of MMOH and MMOB prior to protein reduction by $Na_2S_2O_4$ only increases the product yield from ~80% to ~88% (*38*), a smaller and less significant effect than in PH or ToMO. The reasons for the differences between PH/ToMOH and sMMO are unknown, but because it is likely that the mechanisms of hydrocarbon substrate ingress differ between these systems (*57*), conformational changes in the hydroxylase induced by binding of the electron transfer protein could regulate hydrocarbon substrate entry.

Regulatory Proteins Regulate ET. The present experiments revealed that NADH consumption by PH and ToMO is retarded in the absence of the regulatory protein when this process is rate-determining because hydrocarbon substrate is not present (Table 2). Similar studies have been reported for sMMO (*20*). These results implicate the regulatory protein in the ET process, although the molecular details of this process are not understood. X-ray crystal structures of hydroxylase/regulatory protein complexes from *Pseudomonas* sp. OX1 PH (*31*) and *Pseudomonas mendocina* KR1 T4mo (*30*) show that the regulatory protein binds to the hydroxylase at the proposed docking site of the cognate electron transfer protein. It is likely that the regulatory protein promotes a long-lived conformational change in the hydroxylase that persists after its dissociation and facilitates ET protein binding and/or electron transfer to the hydroxylase diiron centers (*30*). A similar role of the sMMO regulatory protein has been proposed (*32*).

H_2O_2 Generation by BMMs. In the presence of hydrocarbon substrate, H_2O_2 is not produced by PH or ToMO (Scheme 2) because all reducing equivalents are used productively to form hydroxylated product and H_2O (Scheme 2a). In the absence of hydrocarbon substrate, however, PH and ToMO can generate H_2O_2. Under the conditions employed in the experiments, production of H_2O_2 results from the hydroxylase (Scheme 2b), and, in the case of PH, from oxidase activity of the reductase protein (Scheme 2c).

Previous studies probing the reactions of chemically reduced PHH (*17*) or ToMOH (*15*) with O_2 in the presence of the appropriate regulatory protein revealed that long-lived peroxodiiron(III) intermediate species with unique spectroscopic and optical characteristics accumulate and decay to a diiron(III)

product without forming any high-valent iron species (Scheme 3). This species is thought to be responsible for rapid oxidation of hydrocarbon substrate (*15*). Decay of the peroxodiiron(III) transients is expected to occur by protonation and liberation of the bound peroxide unit as H_2O_2 in the absence of hydrocarbon substrate. Consistent with this proposal is the observation that sMMO does not produce H_2O_2 under steady-state conditions (*20*). In this system, the second peroxodiiron(III) intermediate that accumulates, H_{peroxo}, rapidly converts to the di(μ-oxo)diiron(IV) species Q, which can decay by acquiring two electrons and two protons to release H_2O and form the diiron(III) resting state (*20, 58*).

In the context of the cell, the choice of whether the reducing equivalents are used to generate hydroxylated product and H_2O or H_2O_2 is under kinetic control for PH and ToMO: much slower kinetics of H_2O_2 formation (Figure 1) relative to catechol formation (*39, 42*) (Figure S1) ensures that electrons are not used unproductively to generate H_2O_2 when the hydrocarbon substrate is present (Scheme 3). This kinetic effect might reflect a thermodynamic preference of the system for an un- or mono-protonated peroxoiiron(III) species rather than its diprotonated form, enforced by the electrostatic environment of the enzyme active sites. In this manner, the enzymes have evolved to control the product outcome such that only productive hydroxylated product is formed in the presence of hydrocarbon substrate.

CONCLUDING REMARKS

In conclusion, the present experiments reveal that the auxiliary proteins of PH and ToMO affect catalysis in a well-controlled manner. The regulatory proteins PHM and ToMOD accelerate ET, and the ET proteins regulate substrate oxidation. Unraveling the details of the molecular mechanisms underlying these dynamic protein interactions is of crucial importance for understanding these remarkable systems in future studies.

ACKNOWLEDGEMENT

We thank Dr. Rachel K. Behan for helpful discussions.

SUPPORTING INFORMATION

Figures S1-S4 as described in the text (PDF). This material is available free of charge via the Internet at http://pubs.acs.org.

REFERENCES

1. Murray, L. J., and Lippard, S. J. (2007) Substrate Trafficking and Dioxygen Activation in Bacterial Multicomponent Monooxygenases, *Acc. Chem. Res. 40*, 466-474.
2. Sazinsky, M. H., and Lippard, S. J. (2006) Correlating Structure with Function in Bacterial Multicomponent Monooxygenases and Related Diiron Proteins, *Acc. Chem. Res. 39*, 558-566.
3. Leahy, J. G., Batchelor, P. J., and Morcomb, S. M. (2003) Evolution of the Soluble Diiron Monooxygenases, *FEMS Microbiol. Rev. 27*, 449-479.
4. Notomista, E., Lahm, A., Di Donato, A., and Tramontano, A. (2003) Evolution of Bacterial and Archaeal Multicomponent Monooxygenases, *J. Mol. Evol. 56*, 435-445.
5. Wallar, B. J., and Lipscomb, J. D. (1996) Dioxygen Activation by Enzymes Containing Binuclear Non-Heme Iron Clusters, *Chem. Rev. 96*, 2625-2657.
6. Brazeau, B. J., and Lipscomb, J. D. (2000) Kinetics and Activation Thermodynamics of Methane Monooxygenase Compound Q Formation and Reaction with Substrates, *Biochemistry 39*, 13503-13515.
7. Tinberg, C. E., and Lippard, S. J. (2009) Revisiting the Mechanism of Dioxygen Activation in Soluble Methane Monooxygenase from *M. capsulatus* (Bath): Evidence for a Multi-Step, Proton-Dependent Reaction Pathway, *Biochemistry 48*, 12145-12158.
8. Liu, K. E., Valentine, A. M., Wang, D., Huynh, B. H., Edmondson, D. E., Salifoglou, A., and Lippard, S. J. (1995) Kinetic and Spectroscopic Characterization of Intermediates and Component Interactions in Reactions of Methane Monooxygenase from *Methylococcus capsulatus* (Bath), *J. Am. Chem. Soc. 117*, 10174-10185.
9. Liu, K. E., Wang, D., Huynh, B. H., Edmondson, D. E., Salifoglou, A., and Lippard, S. J. (1994) Spectroscopic Detection of Intermediates in the Reaction of Dioxygen with Reduced Methane Monooxygenase Hydroxylase from *Methylococcus capsulatus* (Bath), *J. Am. Chem. Soc. 116*, 7465-7466.

10. Valentine, A. M., Stahl, S. S., and Lippard, S. J. (1999) Mechanistic Studies of the Reaction of Reduced Methane Monooxygenase Hydroxylase with Dioxygen and Substrates, *J. Am. Chem. Soc. 121*, 3876-3887.

11. Lee, S.-K., and Lipscomb, J. D. (1999) Oxygen Activation Catalyzed by Methane Monooxygenase Hydroxylase Component: Proton Delivery during the O—O Bond Cleavage Steps, *Biochemistry 38*, 4423-4432.

12. Lee, S.-K., Fox, B. G., Froland, W. A., Lipscomb, J. D., and Münck, E. (1993) A Transient Intermediate of the Methane Monooxygenase Catalytic Cycle Containing an $Fe^{IV}Fe^{IV}$ Cluster, *J. Am. Chem. Soc. 115*, 6450-6451.

13. Lee, S.-K., Nesheim, J. C., and Lipscomb, J. D. (1993) Transient Intermediates of the Methane Monooxygenase Catalytic Cycle, *J. Biol. Chem. 268*, 21569-21577.

14. Shu, L., Nesheim, J. C., Kauffmann, K., Münck, E., Lipscomb, J. D., and Que, L., Jr. (1997) An $Fe_2^{IV}O_2$ Diamond Core Structure for the Key Intermediate Q of Methane Monooxygenase *Science 275*, 515-518.

15. Murray, L. J., Naik, S. G., Ortillo, D. O., García-Serres, R., Lee, J. K., Huynh, B. H., and Lippard, S. J. (2007) Characterization of the Arene-Oxidizing Intermediate in ToMOH as a Diiron(III) Species, *J. Am. Chem. Soc. 129*, 14500-14510.

16. Murray, L. J., García-Serres, R., Naik, S., Huynh, B. H., and Lippard, S. J. (2006) Dioxygen Activation at Non-Heme Diiron Centers: Characterization of Intermediates in a Mutant Form of Toluene/*o*-Xylene Monooxygenase Hydroxylase, *J. Am. Chem. Soc. 128*, 7458-7459.

17. Izzo, V., Tinberg, C. E., García-Serres, R., Naik, S., Huynh, B. H., and Lippard, S. J. (2010) Manuscript in Preparation.

18. Merkx, M., Kopp, D. A., Sazinsky, M. H., Blazyk, J. L., Müller, J., and Lippard, S. J. (2001) Dioxygen Activation and Methane Hydroxylation by Soluble Methane Monooxygenase: A Tale of Two Irons and Three Proteins, *Angew. Chem. Int. Ed. 40*, 2782-2807.

19. Fox, B. G., Liu, Y., Dege, J. E., and Lipscomb, J. D. (1991) Complex Formation between the Protein Components of Methane Monooxygenase from *Methylosinus trichosporium* OB3b: Identification of Sites of Component Interaction, *J. Biol. Chem. 266*, 540-550.

20. Gassner, G. T., and Lippard, S. J. (1999) Component Interactions in the Soluble Methane Monooxygenase System from *Methylococcus capsulatus* (Bath), *Biochemistry 38*, 12768-12785.

21. Green, J., and Dalton, H. (1985) Protein B of Soluble Methane Monooxygenase from *Methylococcus capsulatus* (Bath): A Novel Regulatory Protein of Enzyme Activity, *J. Biol. Chem. 260*, 15795-15801.

22. Pikus, J. D., Studts, J. M., Achim, C., Kauffmann, K. E., Münck, E., Steffan, R. J., McClay, K., and Fox, B. G. (1996) Recombinant Toluene-4-monooxygenase: Catalytic and Mössbauer Studies of the Purified Diiron and Rieske Components of a Four-Protein Complex, *Biochemistry 35*, 9106-9119.

23. Liu, K. E., and Lippard, S. J. (1991) Redox Properties of the Hydroxylase Component of Methane Monooxygenase from *Methylococcus capsulatus* (Bath): Effects of Protein B, Reductase, and Substrate, *J. Biol. Chem. 266*, 12836-12839.

24. Paulsen, K. E., Liu, Y., Fox, B. G., Lipscomb, J. D., Münck, E., and Stankovich, M. T. (1994) Oxidation-Reduction Potentials of the Methane Monooxygenase Hydroxylase Component from *Methylosinus trichosporium* OB3b, *Biochemistry 33*, 713-722.

25. DeWitt, J. G., Rosenzweig, A. C., Salifoglou, A., Hedman, B., Lippard, S. J., and Hodgson, K. O. (1995) X-ray Absorption Spectroscopic Studies of the Diiron Center in Methane Monooxygenase in the Presence of Substrate and the Coupling Protein of the Enzyme System, *Inorg. Chem. 34*, 2505-2515.

26. Fox, B. G., Hendrich, M. P., Surerus, K. K., Andersson, K. K., Froland, W. A., Lipscomb, J. D., and Münck, E. (1993) Mössbauer, EPR, and ENDOR Studies of the Hydroxylase and Reductase Components of Methane Monooxygenase from *Methylosinus trichosporium* OB3b, *J. Am. Chem. Soc. 115*, 3688-3701.

27. Froland, W. A., Andersson, K. K., Lee, S.-K., Liu, Y., and Lipscomb, J. D. (1992) Methane Monooxgenase Component B and Reductase Alter the Regioselectivity of the Hydroxylase Component-catalyzed Reactions: A Novel Role for Protein-Protein Interactions in an Oxygenase Mechanism, *J. Biol. Chem. 267*, 17588-17597.

28. Mitić, N., Schwartz, J. K., Brazeau, B. J., Lipscomb, J. D., and Solomon, E. I. (2008) CD and MCD Studies of the Effects of Component B Variant Binding on the Biferrous Active Site of Methane Monooxygenase, *Biochemistry 47*, 8386-8397.

29. Pulver, S. C., Froland, W. A., Lipscomb, J. D., and Solomon, E. I. (1997) Ligand Field Circular Dichroism and Magnetic Circular Dichroism Studies of Component B and Substrate Binding to the Hydroxylase Component of Methane Monooxygenase, *J. Am. Chem. Soc. 119*, 387-395.

30. Bailey, L. J., McCoy, J. G., Phillips, G. N., Jr., and Fox, B. G. (2008) Structural Consequences of Effector Protein Complex Formation in a Diiron Hydroxylase, *Proc. Natl. Acad. Sci. USA 105*, 19194-19198.

31. Sazinsky, M. H., Dunten, P. W., McCormick, M. S., Di Donato, A., and Lippard, S. J. (2006) X-ray Structure of a Hydroxylase-Regulatory Protein Complex from a Hydrocarbon-Oxidizing Multicomponent Monooxygenase, *Pseudomonas* sp. OX1 Phenol Hydroxylase, *Biochemistry 45*, 15392-15404.

32. Blazyk, J. L., Gassner, G. T., and Lippard, S. J. (2005) Intermolecular Electron-Transfer Reactions in Soluble Methane Monooxygenase: A Role for Hysteresis in Protein Function, *J. Am. Chem. Soc. 127*, 17364-17376.

33. Gallagher, S. C., Callaghan, A. J., Zhao, J., Dalton, H., and Trewhella, J. (1999) Global Conformational Changes Control the Reactivity of Methane Monooxygenase, *Biochemistry 38*, 6752-6760.

34. Wallar, B. J., and Lipscomb, J. D. (2001) Methane Monooxygenase Component B Mutants Alter the Kinetic Steps Throughout the Catalytic Cycle, *Biochemistry 40*, 2220-2233.

35. Mitchell, K. H., Studts, J. M., and Fox, B. G. (2002) Combined Participation of Hydroxylase Active Site Residues and Effector Protein Binding in a *Para* to *Ortho* Modulation of Toluene 4-Monooxygenase Regiospecificity, *Biochemistry 41*, 3176-3188.

36. Zheng, H., and Lipscomb, J. D. (2005) Regulation of Methane Monooxygenase Catalysis Based on Size Exclusion and Quantum Tunneling, *Biochemistry 45*, 1685-1692.

37. Liu, Y., Nesheim, J. C., Lee, S.-K., and Lipscomb, J. D. (1995) Gating Effects of Component B on Oxygen Activation by the Methane Monooxygenase Hydroxylase Component, *J. Biol. Chem. 270*, 24662-24665.

38. Liu, Y., Nesheim, J. C., Paulsen, K. E., Stankovich, M. T., and Lipscomb, J. D. (1997) Roles of the Methane Monooxygenase Reductase Component in the Regulation of Catalysis, *Biochemistry 36*, 5223-5233.

39. Cafaro, V., Izzo, V., Scognamiglio, R., Notomista, E., Capasso, P., Casbarra, A., Pucci, P., and Di Donato, A. (2004) Phenol Hydroxylase and Toluene/*o*-Xylene Monooxygenase from *Pseudomonas stutzeri* OX1: Interplay between Two Enzymes, *Appl. Environ. Microbiol. 70*, 2211-2219.

40. Powlowski, J., and Shingler, V. (1994) Genetics and Biochemistry of Phenol Degradation by *Pseudomonas* sp. CF600, *Biodegradation 5*, 219-236.

41. Arenghi, F. L. G., Berlanda, D., Galli, E., Sello, G., and Barbieri, P. (2001) Organization and Regulation of *meta* Cleavage Pathway Genes for Toluene and *o*-Xylene Derivative Degradation in *Pseudomonas stutzeri* OX1, *Appl. Environ. Microbiol. 67*, 3304-3308.

42. Cafaro, V., Scognamiglio, R., Viggiani, A., Izzo, V., Passaro, I., Notomista, E., Dal Piaz, F., Amoresano, A., Casbarra, A., Pucci, P., and Di Donato, A. (2002) Expression and Purification of the Recombinant Subunits of Toluene/*o*-Xylene Monooxygeanse and Reconsitution of the Active Complex, *Eur. J. Biochem. 269*, 5689-5699.

43. Bertoni, G., Martino, M., Galli, E., and Barbieri, P. (1998) Analysis of the Gene Cluster Encoding Toluene/*o*-Xylene Monooxygenase from *Pseudomonas stutzeri* OX1, *App. Environ. Microbiol. 64*, 3626-3632.

44. Scognamiglio, R., Notomista, E., Barbieri, P., Pucci, P., Dal Piaz, F., Tramontano, A., and Di Donato, A. (2001) Conformational Analysis of Putative Regulatory Subunit D of the Toluene/*o*-Xylene-Monooxygenase Complex from *Pseudomonas stutzeri* OX1, *Protein Sci. 10*, 482-490.

45. Song, W. J., Behan, R. K., Naik, S. G., Huynh, B. H., and Lippard, S. J. (2009) Characterization of a Peroxodiiron(III) Intermediate in the T201S Variant of Toluene/*o*-Xylene Monooxygenase Hydroxylase from *Pseudomonas* sp. OX1, *J. Am. Chem. Soc. 131*, 6074-6075.

46. Murray, L. J., García-Serres, R., McCormick, M. S., Davydov, R., Naik, S. G., Kim, S.-H., Hoffman, B. M., Huynh, B. H., and Lippard, S. J. (2007) Dioxygen Activation at Non-Heme Diiron Centers: Oxidation of a Proximal Residue in the I100W Variant of Toluene/*o*-Xylene Monooxygenase Hydroxylase, *Biochemistry 46*, 14795-14809.

47. Gibbs, C. R. (1976) Characterization and Application of FerroZine Iron Reagent as a Ferrous Iron Indicator, *Anal. Chem. 48*, 1197-1201.

48. Lambeth, D. O., and Palmer, G. (1973) The Kinetics and Mechanism of Reduction of Electron Transfer Protein and Other Compounds of Biological Interest by Dithionite, *J. Biol. Chem. 248*, 6095-6103.

49. Hildebrandt, A. G., and Roots, I. (1975) Reduced Nicotinamide Adenine Dinucleotide Phosphate (NADPH)- Dependent Formation and Breakdown of Hydrogen Peroxide during Mixed Function Oxidation Reaction in Liver Microsomes, *Arch. Biochem. Biophys. 171*, 385-397.

50. Switala, J., and Loewen, P. C. (2002) Diversity of Properties Among Catalases, *Arch. Biochem. Biophys. 401*, 145-154.

51. Elsen, N. L., Bailey, L. J., Hauser, A. D., and Fox, B. G. (2009) Role for Threonine 201 in the Catalytic Cycle of the Soluble Diiron Hydroxylase Toluene 4-Monooxygenase, *Biochemistry 48*, 3838-3846.

52. Messner, K. R., and Imlay, J. A. (2002) *In Vitro* Quantitation of Biological Superoxide and Hydrogen Peroxide Generation, *Methods Enzymol. 349*, 354-361.

53. Yang, X., and Ma, K. (2005) Determination of Hydrogen Peroxide Generated by Reduced Nicotinamide Adenine Dinucleotide Oxidase, *Anal. Biochem. 344*, 130-134.

54. Newman, L. M., and Wackett, L. P. (1995) Purification and Characterization of Toluene 2-Monooxygenase from *Burkholderia cepacia* G4, *Biochemistry 34*, 14066-14076.

55. Cadieux, E., Vrajmasu, V., Achim, C., Powlowski, J., and Münck, E. (2002) Biochemical, Mössbauer, and EPR Studies of the Diiron Cluster of Phenol Hydroxylase from *Pseudomonas* sp. Strain CF 600, *Biochemistry 41*, 10680-10691.

56. Song, W. J., and Lippard, S. J. (2010) Unpublished Results.

57. McCormick, M. S. (2008) Structural Investigations of Hydroxylase Proteins and Complexes in Bacterial Multicomponent Monooxygenase Systems, Ph.D. Thesis (Massachusetts Institute of Technology, Cambridge, MA).

58. Lund, J., Woodland, M. P., and Dalton, H. (1985) Electron Transfer Reactions in the Soluble Methane Monooxygenase of *Methylococcus capsulatus* (Bath), *Eur. J. Biochem. 147*, 297-305.

Table 1. Single Turnover Yields[a]

Phenol Hydroxylase (PH)			Toluene/*o*-Xylene Monooxygenase (ToMO)		
Reaction Conditions	Reducing Agent	% Catechol Formed/ Active Sites	Reaction Conditions	Reducing Agent	% Catechol Formed/ Active Sites
PHH	$Na_2S_2O_4$	nd[b]	ToMOH	$Na_2S_2O_4$	6.9 ± 0.2
PHH:6PHM:2PHP	NADH	54 ± 2	ToMOH:2ToMOD:2ToMOC:0.1ToMOF	NADH	50 ± 7
PHH:6PHM:2PHP	$Na_2S_2O_4$	54 ± 1	ToMOH:2ToMOD:2ToMOC	$Na_2S_2O_4$	46 ± 3
PHH_{red}:6PHM:$2PHP_{ox}$[c]	$Na_2S_2O_4$	24 ± 6	$ToMOH_{red}$:2ToMOD:$2ToMOC_{ox}$[d]	$Na_2S_2O_4$	29 ± 1
PHH:6PHM	$Na_2S_2O_4$	nd[b]	ToMOH:2ToMOD	$Na_2S_2O_4$	10.0 ± 0.9
PHH:2PHP	$Na_2S_2O_4$	8 ± 3	ToMOH:2ToMOC	$Na_2S_2O_4$	11 ± 2

[a]All experiments were performed at 25 °C. [b]None detected. [c]PHH:6M was pre-reduced with stoichiometric $Na_2S_2O_4$ prior to adding PHP_{ox}. After subsequent addition of O_2-saturated buffer, the solution was assayed for catechol content. [d]ToMOH:2D was pre-reduced with stoichiometric $Na_2S_2O_4$ prior to adding $ToMOC_{ox}$. After subsequent addition of O_2-saturated buffer, the solution was assayed for catechol content.

Table 2. NADH Consumption Rates[a]

Phenol Hydroxylase (PH)		Toluene/*o*-Xylene Monooxygenase (ToMO)	
Reaction Conditions	NADH Consumption Rate (μM/min)	Reaction Conditions	NADH Consumption Rate (μM/min)
PHH	nd[b]	ToMOH	nd[b]
PHH:6PHM:2PHP	67.2 ± 0.7	ToMOH:4ToMOD:2ToMOC:0.1ToMOF	14 ± 2
PHH:2PHP	17.6 ± 0.2	ToMOH:4ToMOD	6.4 ± 0.6
PHH:6PHM:2PHP:phenol	180 ± 7	ToMOH:4ToMOD:2ToMOC:0.1ToMOF:phenol	86 ± 5
2PHP	4.0 ± 0.3	0.1ToMOF:2ToMOC	1.9 ± 0.2

[a]All experiments were performed at 25 °C. [b]No NADH consumption detected.

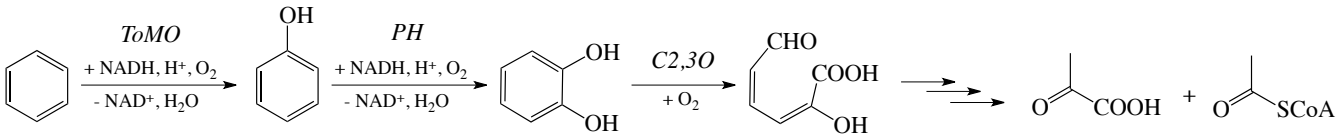

Scheme 1. Pathway of benzene metabolism by *Pseudomonas* sp. OX1.

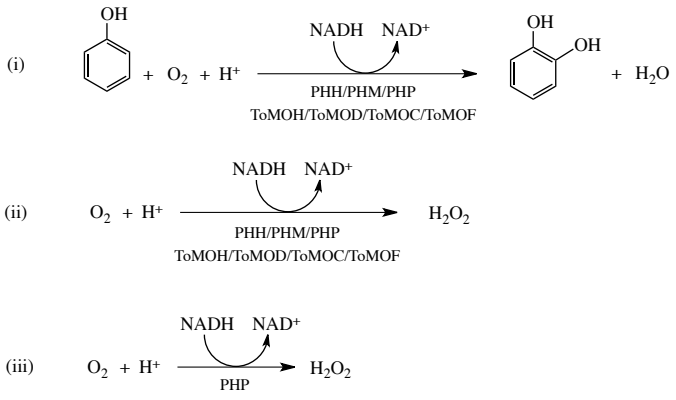

Scheme 2. Product evolution by PH or ToMO in the presence (i) or absence (ii) of phenol and by PHP in the absence of phenol (iii).

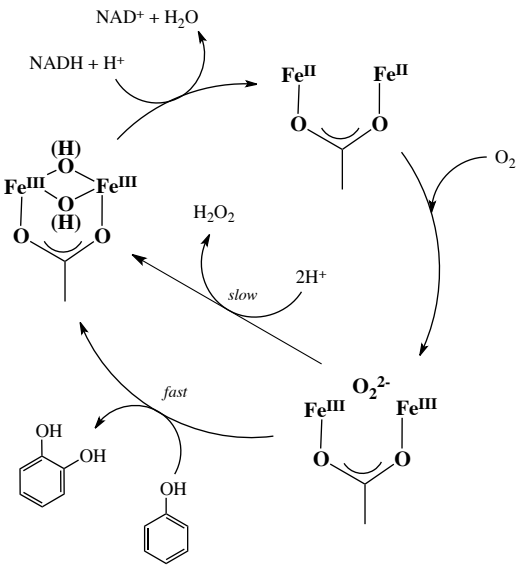

Scheme 3. Proposed mechanism of O_2 activation by ToMO and PH.

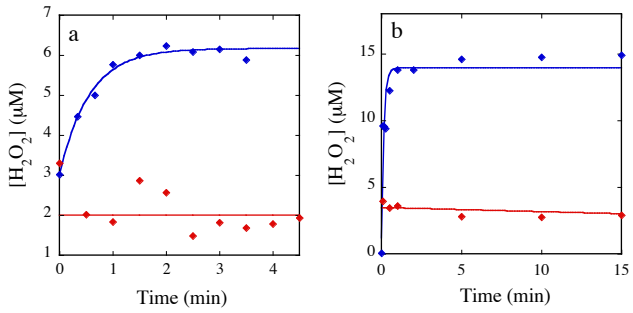

Figure 1. Representative profiles of H_2O_2 generated by PH (a) and ToMO (b). (a) H_2O_2 generation profile upon addition of 200 μM NADH to a solution of 1 μM PHH, 6 μM PHM, 2 μM PHP, and 10 μM NH_2OH at pH 7.5 and 4 °C in the presence (red diamonds) or absence (blue diamonds) of 5 mM phenol. (b) H_2O_2 generation profile upon addition of 200 μM NADH to a solution of 1 μM ToMOH, 2 μM ToMOD, 2 μM ToMOC, 0.1 μM ToMOF, and 10 μM NH_2OH at pH 7.5 and 4 °C in the presence (red diamonds) or absence (blue diamonds) of 5 mM phenol. Data obtained in the absence of phenol were fit (solid lines) to the single exponential formation process y = A*exp(-*k*t) + B. Reaction solutions were assayed for H_2O_2 content as noted in the text.

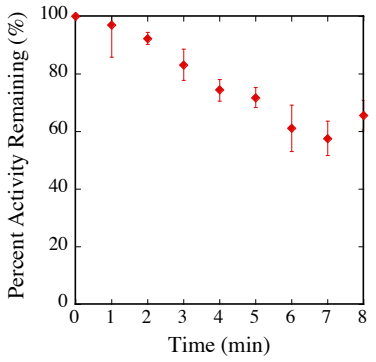

Figure 2. Percent PH activity remaining as a function of time following incubation with NADH. Reaction solutions containing 1 μM PHH, 6 μM PHM, 2 μM PHP in 500 μL of 0.1 M Tris-HCl, pH 7.5, were incubated with 5 mM NADH for a specified time period between 0 and 8 min, after which 5 mM phenol was added. Reactions were allowed to proceed for 20 min and then were quenched by addition of 100 μL of TCA. Catechol content was monitored by HPLC. Data are plotted as the percentage of the amount of catechol formed in experiments in which NADH and phenol were added simultaneously (t = 0 min) versus the time that the reaction mixture was incubated with NADH before addition of phenol. Data points represent the average of two trials performed with different batches of protein.

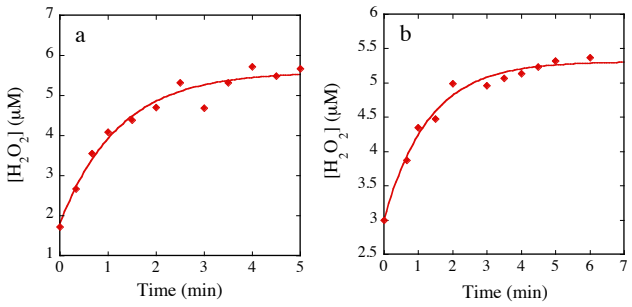

Figure 3. (a) Representative profile of H_2O_2 generation (red diamonds) upon addition of 200 μM NADH to 2 μM PHP at pH 7.5 and 4 °C. Similar reaction profiles were obtained in the presence of NH_2OH. (b) Representative profile of H_2O_2 generation (red diamonds) upon addition of 200 μM NADH to a solution of 1 μM PHH, 6 μM PHM, 0.1 μM PHP, and 10 μM NH_2OH at pH 7.5 and 4 °C. Data were fit (solid lines) to the single exponential formation process y = A*exp(-*k*t) + B. Reaction solutions were assayed for H_2O_2 content as noted in the text. See text for comment on the non-zero ordinate intercepts.

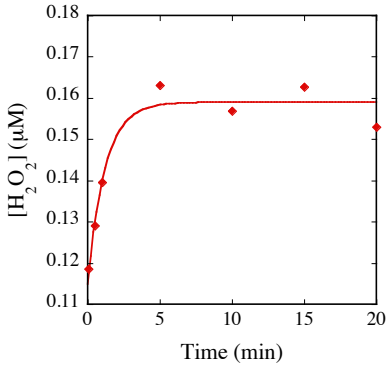

Figure 4. Representative H_2O_2 generation profile upon addition of 200 μM NADH to a solution of 1 μM ToMOH I100W, 2 μM ToMOD, 2 μM ToMOC, 0.1 μM ToMOF, and 10 μM NH_2OH at pH 7.5 and 25 °C in the absence of phenol. Data were fit (solid lines) to a single exponential formation process, $y = A*\exp(-kt) + B$. Reaction solutions were assayed for H_2O_2 content as noted in the text.

For Table of Contents Use Only:

Multiple Roles of Component Proteins in Bacterial Multicomponent Monooxygenases: Phenol Hydroxylase and Toluene/*o*-Xylene Monooxygenase from *Pseudomonas* sp. OX1

Christine E. Tinberg, Woon Ju Song, Viviana Izzo, and Stephen J. Lippard*

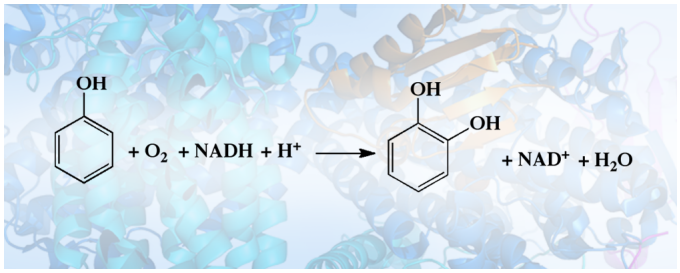

TOC Graphic